

Effective bridge spectral density for long-range biological energy and charge transfer

Oliver Kühn, Valery Rupasov,^{a)} and Shaul Mukamel
Department of Chemistry, University of Rochester, Rochester, New York 14627

(Received 18 September 1995; accepted 9 January 1996)

The role of medium-induced relaxation of intermediate (bridge) sites in energy and charge transfer processes in molecular aggregates of arbitrary size and geometry is explored by means of Green's function techniques. The coupling of electronic and (solvent and intramolecular) nuclear degrees of freedom is incorporated using the Brownian oscillator model, which allows an exact calculation of the necessary two-point and four-point correlation functions of exciton operators. The signatures of energy transfer and spectral diffusion in time- and frequency-resolved fluorescence spectroscopy are studied. A unified expression for the frequency-dependent transfer rate is derived, which interpolates between the sequential and superexchange limits. Numerical results and a Liouville space pathway analysis for a donor-acceptor system coupled through a single bridge molecule are presented.
© 1996 American Institute of Physics. [S0021-9606(96)00115-2]

I. INTRODUCTION

Many important chemical and biological processes involve long-range transfer of electronic excitation energy or electric charges between donor and acceptor molecules.¹⁻⁹ At large spatial separation, there is no direct donor-acceptor (DA) coupling, and intervening "bridge" sites that promote the transfer are required. One of the key questions in the study of donor-bridge-acceptor complexes is the nature of the transfer process, which could be either a sequential (incoherent) hopping between adjacent sites or a direct quantum tunneling (superexchange) between the donor and the acceptor. In the former case the bridge provides intermediate sites in which the excitation resides, whereas the only role of the bridge in the latter case is to provide virtual orbitals that determine the effective DA coupling. These mechanisms have been discussed in connection with ultrafast biological electron transfer in the reaction center (RC) of photosynthetic systems,¹⁰⁻¹⁶ which may be modeled as a three-site system, where the electron moves 17 Å in ~3 ps. Ultrafast DA-electron transfer through a DNA helix has been reported⁵ and investigated theoretically¹⁷ as well. Here an electron requires several nanoseconds to travel more than 40 Å.

Recent structural data on the light harvesting antennae of bacterial RCs¹⁸ and of the RC of higher plants¹⁹ have triggered a host of nonlinear optical studies of the energy transfer mechanism. In the chlorophyll *a/b* protein antenna complex of Photosystem II, for instance, transient absorption spectroscopy revealed a dynamics involving several pigment molecules before the excitation energy is finally trapped in the acceptor state.²⁰ Time-resolved fluorescence is a valuable tool in the study of energy transfer mechanisms in molecular aggregates and crystals.^{21,22} Considerable insight has been gained recently into the role of different system time scales

in light harvesting antennae.^{23,24} Effects such as spectral diffusion, excitation equilibration, and the role of protein modes have been discussed in great detail. Hole burning,²⁵ pump-probe,²⁶ and photon echo²⁷ spectroscopies have been used as well. Coupling with the medium (protein, solvent, and chromophore's nuclear motions) is crucial in determining the transfer rates and pathways. In the superexchange limit the problem reduces to an effective two-site system, and the medium only enters through its coupling to the donor and acceptor. This is the standard charge transfer problem, which can be handled by the Marcus theory,²⁸ where solvent motions are incorporated via a single solvation coordinate. Formally, this is equivalent to the calculation of an ordinary absorption lineshape. When the intermediate bridge states are resonant or near resonant with the donor and acceptor, the medium effects on the bridge need to be included as well. A simple way to treat bath-induced dephasing processes is given by the Haken-Strobl model.²⁹⁻³³ This is an infinite temperature model that does not allow the incorporation of an arbitrary spectral density of the medium. Such spectral densities are currently available experimentally and theoretically.³³⁻³⁶ The polaron model has been used to study sequential charge and energy transport in crystals.³⁷⁻⁴¹

A unified description that includes sequential and tunneling processes as limiting cases has been developed by formulating the problem using the density matrix and its evolution in Liouville space. A generalized master equation describing the population dynamics of excitons has been derived. A proper incorporation of solvent effects requires the calculation of simultaneous dynamics of several solvation coordinates. Hu and Mukamel¹¹ have calculated the frequency-dependent rates in a three-site system in the static limit for the solvent. Skourtis and Mukamel⁴² have recently analyzed the mechanism for a system with an arbitrary number of bridge sites but without the incorporation of the solvent. In this paper we generalize these studies and examine the effect of a medium with an arbitrary spectral density that is coupled to all sites (donor, acceptor, and bridge) on the

^{a)}On leave from Landau Institute for Theoretical Physics, Kosygina Street 2, 117334 Moscow, and the Institute of Spectroscopy, Russian Academy of Sciences, 142092 Troitsk, Moscow Region, Russia.

dynamics of energy and charge transfer processes in molecular aggregates. In Sec. II we introduce the Frenkel Hamiltonian in the Heitler–London approximation, and present the Green's function formal expressions for the two-point correlation function of exciton operators in the Heisenberg picture. These two-point correlation functions are then related to a hierarchy of two-point and four-point correlation functions of individual (noninteracting) molecules. These are evaluated using the Brownian oscillator model of nuclear dynamics. Numerical calculations of time-resolved fluorescence spectra that demonstrate the role of the finite nuclear motion time scale are presented in Sec. III.

In Sec. IV the frequency-dependent rate matrix is calculated to lowest order in intermolecular interactions and the role of the bridge spectral density is explored. In the sequential limit, the Förster rate is recovered, whereas in the superexchange limit the bridge states enter only through an effective coupling matrix element between donor and acceptor. Finally, the frequency-dependent rate in a three-site (single bridge) system is calculated in Sec. V. We formulate the DA transfer in terms of Liouville space pathways,¹¹ which have been widely used in nonlinear optics⁴³ as well as electron transfer theory.^{44,42} The various Liouville space pathways are discussed and used to identify the sequential and superexchange contributions to the transfer. The results generalize the static limit expressions of Hu and Mukamel¹¹ for electron transfer to incorporate solvation processes with arbitrary time scales.

II. CORRELATION FUNCTION EXPRESSIONS FOR ENERGY TRANSFER

In this section we introduce the Hamiltonian and review the iterative correlation function procedure for calculating the excitation transfer developed by Mukamel and Rupasov.⁴⁵ For clarity we focus on energy transfer. However, the quantities calculated can be used for the description of charge transfer as well, as will be shown in Sec. IV.

We consider a molecular aggregate consisting of N molecules, described by the Frenkel exciton Hamiltonian,^{21,46}

$$H = H_0 + V + H_F(t), \quad (1)$$

where H_0 represents noninteracting molecules, each assumed to be an electronic two-level system with a ground state $|g\rangle$ and an excited state $|e\rangle$,

$$H_0 = \sum_{n=1}^N H_n(\mathbf{q}) B_n^+ B_n + H_{\text{nuc}}(\mathbf{q}). \quad (2)$$

The operators B_n^+ (B_n) that create (annihilate) an electronic excitation on the n th molecule, satisfy the Pauli commutation rules:

$$[B_n, B_m^+] = \delta_{nm}(1 - 2B_n^+ B_n). \quad (3)$$

$H_{\text{nuc}}(\mathbf{q})$ is the nuclear Hamiltonian that describes intramolecular as well as solvent degrees of the freedom, denoted \mathbf{q} . The coupling of electronic and nuclear degrees of freedom is represented by $H_n(\mathbf{q})$ which accounts for the change in the

nuclear Hamiltonian upon excitation of site n . The second term in Eq. (1) represents intermolecular dipole–dipole coupling, and is given by

$$V = \sum_{nm} v_{nm} (B_n^+ B_m + B_m^+ B_n). \quad (4)$$

We assume that only one molecule (the donor, labeled $n=1$) interacts with the external electric field $E(t)$. Thus, $H_F(t)$ is

$$H_F(t) = -\mu_1 [E(t) B_1^+ + E^*(t) B_1], \quad (5)$$

where μ_1 is its transition dipole moment. We further invoke the Condon approximation for the dipole moment as well as for the intermolecular coupling and neglect their dependence on the nuclear configuration.

Using this Hamiltonian, we shall calculate the two-point correlation function,

$$\tilde{\sigma}_n(t, t') = \langle \tilde{B}_n^+(t) \tilde{B}_n(t') \rangle, \quad (6)$$

where $\langle \dots \rangle = \text{Tr}\{\dots e^{-H/k_B T}\} / \text{Tr}\{e^{-H/k_B T}\}$, and

$$\tilde{B}_n(t) = U^+(t, -\infty) B_n U(t, -\infty), \quad (7)$$

is the exciton operator in the Heisenberg representation. $U(t, t')$ is the time evolution operator,

$$U(t, -\infty) = \overrightarrow{T} \exp \left[-\frac{i}{\hbar} (H_0 + V)t - \frac{i}{\hbar} \int_{-\infty}^t d\tau H_F(\tau) \right]. \quad (8)$$

The operators \overrightarrow{T} and \overleftarrow{T} stand for chronological and anti-chronological time ordering, respectively. The correlation function (6) carries the information necessary for calculating optical properties and energy transfer processes in the system. This will be illustrated in the coming sections, where we connect it to various observables.

We restrict the following analysis to a single path, where molecule 1 is coupled to 2, 2 to 3, etc., and molecule $N-1$ to N . A perturbative expansion to lowest nonvanishing order in the external field and the intermolecular coupling yields

$$\begin{aligned} \tilde{\sigma}_N(t, t') &= \left(\frac{\mu_1}{\hbar} \right)^2 \left[\prod_{n=2}^N \left(\frac{v_{n,n-1}}{\hbar} \right) \right]^2 \int_{-\infty}^t dt_{N-1} \cdots dt_1 d\tau \\ &\times \int_{-\infty}^{t'} dt'_{N-1} \cdots dt'_1 d\tau' E^*(\tau) E(\tau') \\ &\times \langle \overrightarrow{T} [B_1(\tau) B_1^+(t_1) \cdots B_N(t_{N-1}) B_N^+(t)] \\ &\times \overleftarrow{T} [B_N(t') B_N^+(t'_{N-1}) \cdots B_1(t'_1) B_1^+(\tau')] \rangle. \end{aligned} \quad (9)$$

We now assume that each molecule is coupled to a different set of nuclear degrees of freedom and that nuclear dynamics of different molecules are uncorrelated. This implies that H_n depends on \mathbf{q}_n , which is a subset of the entire nuclear degrees of freedom \mathbf{q} . Using this model, we can construct a numerically efficient iterative procedure for computing the necessary correlation functions. We first calculate the

donor correlation function,

$$\begin{aligned} \tilde{\sigma}_1(t, t') &= \left(\frac{\mu_1}{\hbar}\right)^2 \int_{-\infty}^t d\tau \int_{-\infty}^{t'} d\tau' \Gamma_1(\tau, t, t', \tau') E^*(\tau) E(\tau'). \end{aligned} \quad (10)$$

The remaining (bridge and acceptor) correlation functions are then obtained successively through the recursive relation

$$\begin{aligned} \tilde{\sigma}_n(t, t') &= \left(\frac{v_{n,n-1}}{\hbar}\right)^2 \int_{-\infty}^t d\tau \int_{-\infty}^{t'} d\tau' \Gamma_n(\tau, t, t', \tau') \\ &\times \tilde{\sigma}_{n-1}(\tau, \tau') \quad (n = 2 \cdots N). \end{aligned} \quad (11)$$

The molecular correlation function that appears in these expressions is given by

$$\Gamma_n(t_1, t_2, t_3, t_4) = \langle B_n(t_1) B_n^\dagger(t_2) B_n(t_3) B_n^\dagger(t_4) \rangle. \quad (12)$$

Here $B_n(t)$ denotes the time-dependent exciton operator in the interaction representation, i.e.,

$$B_n(t) = e^{iH_0 t/\hbar} B_n e^{-iH_0 t/\hbar}, \quad (13)$$

and $\langle \cdots \rangle = \text{Tr}\{\cdots e^{-H_0/k_B T}\} / \text{Tr}\{e^{-H_0/k_B T}\}$. We shall also define the two-time correlation functions,

$$\sigma_n(t' - t) = \langle B_n(t') B_n^\dagger(t) \rangle. \quad (14)$$

In what follows we represent the solvent using the Brownian oscillator model. In this model, nuclear motions that couple to the electronic transition are treated as a continuous distribution of harmonic modes whose equilibrium positions are displaced between the two electronic states.⁴³ The nuclear Hamiltonian assumes the form $H_{\text{nuc}} = \sum_j \hbar \omega_{j,n} b_{j,n}^\dagger b_{j,n}$, and $H_n = \hbar(\Omega_n + \lambda_n) + (1/\sqrt{2}) \times \sum_j \hbar \omega_{j,n} d_{j,n} (b_{j,n}^\dagger + b_{j,n})$, where Ω_n is the electronic transition frequency and $\omega_{j,n}$, $d_{j,n}$ are the frequency and the dimensionless displacement of the j th oscillator, and $b_{j,n}^\dagger$ ($b_{j,n}$) is its creation (annihilation) operator. We further introduce the reorganization energy (Stokes shift parameter) $\lambda_n = 1/2 \sum_j d_{j,n}^2 \omega_{j,n}$. For this model, the two- and four-point correlation functions are⁴³

$$\sigma_n(t' - t) = \exp\{-i(\Omega_n + \lambda_n)(t' - t) - g_n(t' - t)\} \quad (15)$$

and

$$\begin{aligned} \Gamma_n(t_1, t_2, t_3, t_4) &= \exp\{-i(\Omega_n + \lambda_n)(t_1 - t_2 + t_3 - t_4) - F_n(t_1, t_2, t_3, t_4)\}, \end{aligned} \quad (16)$$

where

$$\begin{aligned} F_n(t_1, t_2, t_3, t_4) &= g_n(t_1 - t_2) + g_n(t_2 - t_3) + g_n(t_1 - t_4) \\ &+ g_n(t_3 - t_4) - g_n(t_1 - t_3) - g_n(t_2 - t_4). \end{aligned} \quad (17)$$

The function $g_n(t)$ is given by

$$\begin{aligned} g_n(t) &= - \int_{-\infty}^{\infty} \frac{d\omega}{2\pi} \frac{C_n(\omega)}{\omega^2} \\ &\times \left[(1 - \cos(\omega t)) \coth\left(\frac{\hbar\omega}{2k_B T}\right) - i(\sin(\omega t) - \omega t) \right], \end{aligned} \quad (18)$$

where $C_n(\omega)$ is the *spectral density* associated with nuclear (solvent and intramolecular) dynamics,

$$C_n(\omega) = \frac{1}{2} \sum_j \omega_{j,n}^2 d_{j,n}^2 [\delta(\omega - \omega_{j,n}) - \delta(\omega + \omega_{j,n})]. \quad (19)$$

These expressions will be applied in the coming sections for calculating the time- and frequency-resolved fluorescence as well as the energy and charge transfer rates in molecular aggregates.

III. APPLICATION TO TIME- AND FREQUENCY-RESOLVED FLUORESCENCE SPECTROSCOPY

In the following we adopt the overdamped Brownian oscillator model for the spectral density, i.e.,

$$C_n(\omega) = 2\lambda_n \frac{\omega \Lambda_n}{\omega^2 + \Lambda_n^2}. \quad (20)$$

In the high-temperature limit, $k_B T \gg \hbar \Lambda_n$, Eqs. (18) and (20) yield

$$g_n(t) = \left(\frac{\Delta_n^2}{\Lambda_n^2} - i \frac{\lambda_n}{\Lambda_n} \text{sgn}(t) \right) (e^{-\Lambda_n |t|} + \Lambda_n |t| - 1), \quad (21)$$

with

$$\Delta_n = \sqrt{2\lambda_n k_B T / \hbar}. \quad (22)$$

The two-point correlation functions introduced in the previous section may be used to calculate several interesting spectroscopic observables. (All quantities are given to lowest nonvanishing order in intermolecular coupling and field.) The linear absorption lineshape is

$$\sigma_{\text{abs}}(\omega) = \sum_{n=1}^N \left(\frac{\mu_n}{\hbar} \right)^2 \sigma_n(\omega), \quad (23)$$

where

$$\sigma_n(\omega) = \int_{-\infty}^{\infty} dt e^{i\omega t} \sigma_n(t) \quad (24)$$

is the normalized absorption line shape $[(2\pi)^{-1} \int d\omega \sigma_n(\omega) = 1]$. The full width at half maximum (FWHM) Γ_n of the $\sigma_n(\omega)$ is given by the Padé approximation,⁴³

$$\Gamma_n = \Delta_n \frac{2.355 + 1.76\kappa_n}{1 + 0.85\kappa_n + 0.88\kappa_n^2}, \quad (25)$$

where the dimensionless parameter $\kappa_n \equiv \Lambda_n / \Delta_n$ determines the nature of the line shape; for $\kappa_n \ll 1$ it assumes a Gaussian inhomogeneous form, whereas for $\kappa_n \gg 1$ it becomes a motionally narrowed Lorentzian.

The relaxed fluorescence signal is

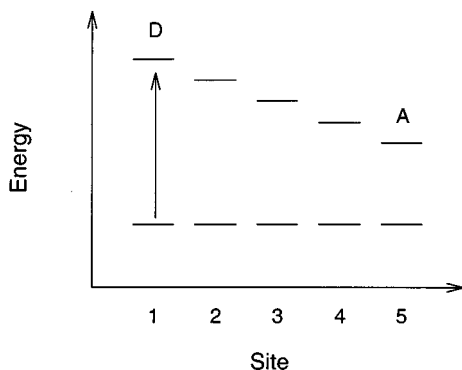


FIG. 1. Energy level scheme for the five monomer aggregate used in the calculation of the time- and frequency-resolved fluorescence. The transition energies are $\hbar(\Omega_n - \Omega_5) = (5 - n) \times 0.02$ eV and the Stokes shift is $\hbar\lambda_n = 0.01$ eV for all molecules. The arrow indicates that the external field only excites the donor ($n = 1$) molecule.

$$\sigma_{\text{fl}}(\omega) = 2\pi\omega \sum_{n=1}^N P_n \sigma'_n(\omega), \quad (26)$$

with the normalized fluorescence line shape

$$\sigma'_n(\omega) = \int_{-\infty}^{\infty} dt e^{i\omega t} \sigma'_n(t). \quad (27)$$

Here $\sigma'_n(t)$ is the correlation function, Eq. (14), with the only difference that it is calculated with respect to the density matrix of the excited state and P_n denotes the equilibrium population of site n .

In the following numerical calculations we consider an aggregate with five monomers (Fig. 1) and electronic transition energies $\hbar(\Omega_n - \Omega_5) = (5 - n) \times 0.02$ eV ($n = 1 \dots 4$). We include a single overdamped mode in the high-temperature limit [Eqs. (21)] for each site. Assuming a Stokes shift parameter of $\hbar\lambda_n = 0.01$ eV for all sites and a temperature of $T = 300$ K we have for the coupling strength $\hbar\Delta_n = 0.0227$ eV according to Eq. (22), $\kappa_n = 0.1$, and FWHM $\Gamma_n = 0.0526$ eV [Eq. (25)]. In Fig. 2 we display the

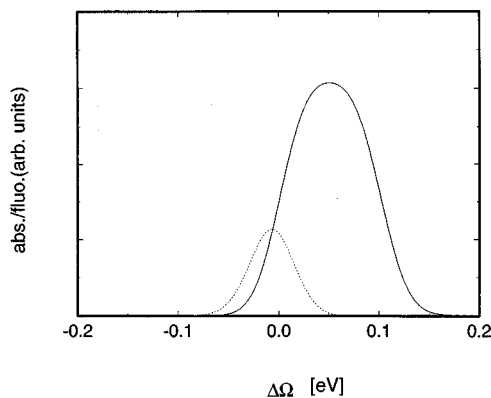
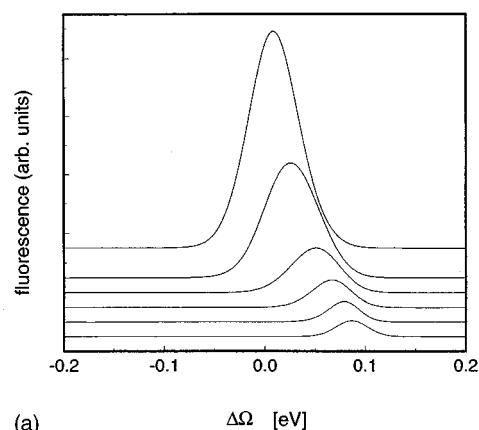
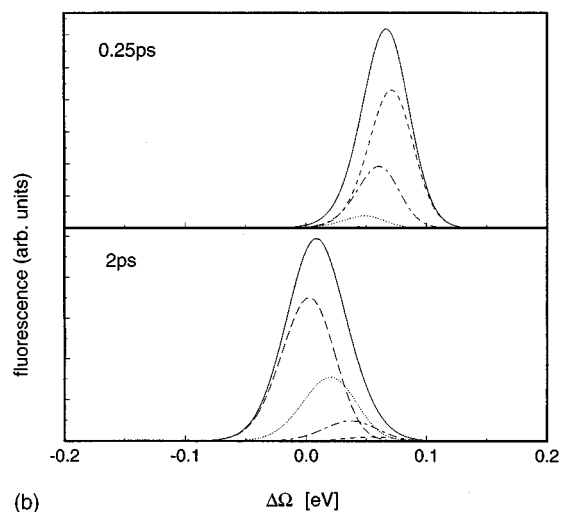


FIG. 2. Stationary absorption [solid line, Eq. (23)] and fluorescence [dashed line, Eq. (23)] spectrum for the aggregate shown in Fig. 1 ($\Delta\Omega = \hbar\omega - \hbar\Omega_5$). The dipole moments of the monomers are assumed to be identical and at equilibrium only the acceptor contributes to the fluorescence. The temperature is $T = 300$ K.



(a)



(b)

FIG. 3. (a) Time-resolved fluorescence spectrum [Eq. (28)] ($\Delta\Omega = \Omega_5 - \omega$) for delay times of 0, 100, 250, 500, 1000, and 2000 fs (from bottom to top, $\Lambda_n = 0.1\Delta_n$). The curves have been shifted vertically and the magnitude was scaled to comprise all delay times (compare Fig. 4). Note that the intramolecular coupling as well as the amplitude of the external field enter Eq. (28) only as an overall scaling factor. (b) The contributions of the individual molecules to the fluorescence spectrum at a delay of 250 fs (top) and 2000 fs (bottom) (solid—total signal; short dashes—2; dashed—dotted—3; dotted—4; and long dashes—5).

stationary absorption of the aggregate (Eq. (23)). The relaxed fluorescence spectrum obtained from Eq. (26) is shown as well, assuming that only the acceptor site is populated at thermal equilibrium.

The time- and frequency-resolved fluorescence of the aggregate, following an excitation pulse that only interacts with molecule 1 (the donor)⁴⁷ is given by^{22,45}

$$S_{\text{fl}}(\omega, t) = 2\pi\omega \sum_{n=1}^N \int_{-\infty}^{\infty} d\tau e^{i\omega\tau} \tilde{\sigma}_n \left(t + \frac{\tau}{2}, t - \frac{\tau}{2} \right). \quad (28)$$

At long times this reduces to the relaxed fluorescence [Eq. (26)].⁴⁵ Fig. 3(a) shows the time-dependent fluorescence spectrum [Eq. (28)]. For clarity, only the fluorescence due to the bridge and the acceptor molecules is displayed in the following calculations; the strong donor emission is not shown. We used a 50 fs Gaussian pulse tuned on resonance

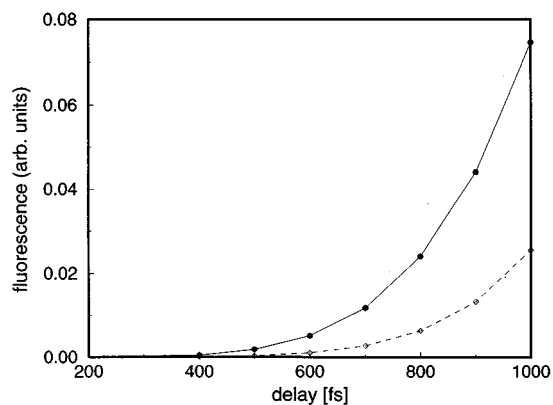


FIG. 4. The time-resolved fluorescence at a fixed frequency $\omega = \Omega_5 - \lambda_5$. $\hbar\lambda_n = 0.01$ eV and $\Gamma_n = 0.0526$ eV; (solid line— $\kappa_n = 0.1$, $\hbar\Delta_n = 0.0227$ eV ($T = 300$ K); dashed line— $\kappa_n = 0.05$, $\hbar\Delta_n = 0.0225$ eV ($T = 294$ K).

with the donor absorption maximum. The correlation functions for the monomers have been calculated iteratively using Eqs. (9)–(11) on a two-dimensional grid with a spacing of 2 fs. The necessary grid size is determined by Δ_n^{-1} as well as the delay time. The maximum grid size was 1200×1200 .

For zero delay the fluorescence coincides with the donor absorption spectrum centered at $\Delta\Omega = 0.09$ eV. For short delays the fluorescence is mainly due to the $n = 2$ bridge molecule that is next to the donor site. With increasing delay the energy is transferred to the acceptor, resulting in a spectral diffusion process. In addition, the spectrum broadens as more sites participate in the emission. The contributions of the individual molecules to the total fluorescence spectrum are plotted in Fig. 3(b) for two delay times. Note that the perturbative approach used here is only valid for short delay times ($t < \hbar/V_{mn}$) (see Sec. IV). In Fig. 4 the rise of the fluorescence at the acceptor frequency ($\omega = \Omega_5 - \lambda_5$) is shown as the parameter κ_n is varied, keeping the FWHM [Eq. (25)] fixed ($\hbar\Gamma_n = 0.0526$ eV). As expected, the acceptor fluorescence rise time slows down as κ_n is decreased.

IV. THE FREQUENCY-DEPENDENT TRANSFER RATE

The previous calculations of the two-time correlation functions $\tilde{\sigma}_n(t, t')$ were carried out to lowest nonvanishing order in intermolecular coupling. As such, they only hold for short times and may not be used to describe the long-time limit. It is possible to extend their range of validity by solving the following integral equations for $\tilde{\sigma}_n(t, t')$ self-consistently rather than iteratively:⁴⁵

$$\begin{aligned} \tilde{\sigma}_n(t, t') &= \sum_{m \neq n} \left(\frac{v_{nm}}{\hbar} \right)^2 \int_{-\infty}^t \int_{-\infty}^{t'} d\tau d\tau' \Gamma_n(\tau, t, t', \tau') \tilde{\sigma}_m(\tau, \tau') \\ &+ \left(\frac{\mu_n}{\hbar} \right)^2 \int_{-\infty}^t \int_{-\infty}^{t'} d\tau d\tau' \Gamma_n(\tau, t, t', \tau') E_n^*(\tau) E_n(\tau'). \end{aligned} \quad (29)$$

In this section we adopt a different procedure and calculate the time-dependent populations of the various molecules, $P_n(t) \equiv \langle \hat{B}_n^+(t) \hat{B}_n(t) \rangle$. These carry less information than the two-point correlation functions, and their simplicity makes it possible to develop a resummed approximation, as will be shown below. Moreover, all the results of the present section apply equally to charge transfer. In the latter case, B_n^+ creates an electron on the n th site, and the two states of each site, $|e\rangle$ and $|g\rangle$ represent a state with and without an electron.⁴⁸ For brevity, we continue to refer to the process as energy transfer. The Hamiltonian is given by $H = H_0 + V$ and we set $H_F = 0$. Thus, we do not incorporate the coupling with the radiation field explicitly, but assume that the system is initially excited, and the nuclear degrees of freedom at each site are equilibrated. The vector $\mathbf{P}(t) = [P_1(t), \dots, P_N(t)]$ satisfies the generalized master equation^{49,50}

$$\frac{d\mathbf{P}(t)}{dt} = \int_0^t d\tau \mathbf{K}(t-\tau) \mathbf{P}(\tau), \quad (30)$$

where $\mathbf{K}(t)$ is the rate matrix. The probabilities $\mathbf{P}(t)$ obtained by solving Eq. (30), when $\mathbf{K}(t)$ is calculated perturbatively, then contain terms to infinite order in intermolecular coupling. Hence, the calculation may hold at long times as well.

We start our calculation of $\mathbf{K}(t)$ by considering the formal solution of Eq. (30),

$$\mathbf{P}(t) = \mathbf{W}(t) \mathbf{P}(0). \quad (31)$$

We further define the Laplace transform of a time-dependent function,

$$A(s) = \int_0^\infty dt A(t) e^{-st}. \quad (32)$$

By applying this transform to Eqs. (30) and (31) we obtain the exact formal relation

$$\mathbf{W}(s) = \frac{1}{s\mathbf{1} - \mathbf{K}(s)}. \quad (33)$$

Expanding both sides of this equation in powers of the intermolecular interaction yields the following recursive relations among the elements of both matrices,⁴⁴

$$K_{mn}^{(2)}(s) = s^2 W_{mn}^{(2)}(s), \quad (34)$$

$$K_{mn}^{(4)}(s) = s^2 W_{mn}^{(4)}(s) - s^3 \sum_l W_{ml}^{(2)}(s) W_{ln}^{(2)}(s), \quad (35)$$

and more generally,

$$\begin{aligned} [\mathbf{K}^{(p)}(s)]_{mn} &= s^2 [\mathbf{W}^{(p)}(s)]_{mn} - s \sum_{q=2,4,\dots}^{p-2} [\mathbf{K}^{(p-q)}(s) \mathbf{W}^{(q)}(s)]_{mn} \\ &\quad (p = 2, 4, \dots), \end{aligned} \quad (36)$$

where p denotes the order in intermolecular coupling and $\mathbf{K}^{(0)} = 0$. Thus, the present procedure consists of calculating $\mathbf{W}(s)$ perturbatively and then using Eq. (36) to get a perturbative expression for the frequency-dependent rate matrix

$\mathbf{K}(s)$. If the intramolecular nuclear dynamics time scale is much faster than the intermolecular transfer time, the rate matrix will show no dispersion in the relevant frequency range, and we can replace $\mathbf{K}(s)$ by $\mathbf{K}=\mathbf{K}(s=0)$. The master equation (30) then becomes an ordinary rate equation $d\mathbf{P}(t)/dt=\mathbf{K}\mathbf{P}(t)$.

The matrix elements $W_{mn}(t)$ give the conditional probability of the system to be in the state m at time t , given that it started at state n at $t=0$, with the nuclear degrees of freedom at thermal equilibrium. They can be calculated using the quantities introduced in the previous section. The only difference is that at $t=0$ the system is now assumed to be with probability one in the excited donor state (n) with the nuclear degrees of freedom at equilibrium. Thus, we can express Eq. (10) in terms of the correlation function that corresponds to the fluorescence spectrum [Eq. (27)] of the donor,

$$\tilde{\sigma}_n(t, t') = \theta(t)\theta(t')\sigma'_n(t' - t), \quad (37)$$

where $\theta(t)$ is the Heaviside step function. Next, we use Eq. (11) to successively calculate $\tilde{\sigma}_{n+1}$, then $\tilde{\sigma}_{n+2}, \dots, \tilde{\sigma}_{m-1}$. Finally, we apply Eq. (11) once more but set $t=t'$, i.e., at the final site (m) we calculate a population rather than the two-point correlation function. We then get

$$W_{mn}^{(2(m-n))}(t) = \left(\frac{v_{m,m-1}}{\hbar}\right)^2 \int_0^t d\tau \int_0^t d\tau' \sigma_m(\tau - \tau') \tilde{\sigma}_{m-1}(\tau, \tau'). \quad (38)$$

Equations (11), (37), and (38) constitute our general expression for the conditional probability to lowest order in v_{mn} . We shall now recast Eq. (38) in a form that clearly

highlights the separate role of the bridge and the DA spectral densities. Combining Eqs. (10), (11), and (38) we get

$$\begin{aligned} W_{mn}^{(2(m-n))}(t) &= \left[\prod_{k=n+1}^m \left(\frac{v_{k,k-1}}{\hbar}\right)^2 \right] \int_0^t dt_m \int_{-\infty}^{t_m} dt_{m-1} \cdots \int_{-\infty}^{t_{n+2}} dt_{n+1} \\ &\times \int_0^t dt'_m \int_{-\infty}^{t'_m} dt'_{m-1} \cdots \int_{-\infty}^{t'_{n+2}} dt'_{n+1} \sigma_m(t_m - t'_m) \\ &\times \Gamma_{m-1}(t_{m-1}, t_m, t'_m, t'_{m-1}) \cdots \\ &\times \Gamma_{n+1}(t_{n+1}, t_{n+2}, t'_{n+2}, t'_{n+1}) \sigma'_n(t'_{n+1} - t_{n+1}). \end{aligned} \quad (39)$$

Next, we introduce the Fourier transform of the four-point correlation functions according to

$$\begin{aligned} \Gamma_k(t_k, t_{k+1}, t'_{k+1}, t'_k) &= \int_{-\infty}^{\infty} \frac{d\omega_k d\omega'_k d\bar{\omega}_k}{(2\pi)^3} \\ &\times e^{-i\omega_k(t_k - t'_k)} e^{-i\omega'_k(t'_{k+1} - t_{k+1})} \\ &\times e^{-i\bar{\omega}_k(t_k + t'_k - t'_{k+1} - t_{k+1})/2} \\ &\times \Gamma_k(\omega_k, \omega'_k, \bar{\omega}_k). \end{aligned} \quad (40)$$

Substituting this in Eq. (39) and performing the time integrations finally yields

$$\begin{aligned} W_{mn}^{(2(m-n))}(s) &= \frac{1}{s^2} \left[\prod_{k=n+1}^m \left(\frac{v_{k,k-1}}{\hbar}\right)^2 \right] \int_{-\infty}^{\infty} \frac{d\omega_m d\omega_n}{(2\pi)^2} \\ &\times \sigma_m(\omega_m) S_{mn}(\omega_m, \omega_n; s) \sigma'_n(\omega_n), \end{aligned} \quad (41)$$

with the bridge spectral function

$$\begin{aligned} S_{mn}(\omega_m, \omega_n; s) &= 2\pi \int_{-\infty}^{\infty} \frac{d\omega_{m-1} d\omega'_{m-1} d\bar{\omega}_{m-1} \cdots d\omega_{n+1} d\omega'_{n+1} d\bar{\omega}_{n+1}}{(2\pi)^3 \cdots (2\pi)^3} \\ &\times \left[\prod_{k=n+1}^{m-1} \frac{\Gamma_k(\omega_k, \omega'_k, \bar{\omega}_k)}{(\omega_k + \bar{\omega}_k/2 + \xi_+(k, n) - \omega_n)(\omega_k - \bar{\omega}_k/2 + \xi_-(k, n) - \omega_n)} \right] \frac{s/\pi}{s^2 + (\omega_m - \omega'_{m-1} + \omega_{m-1} - \cdots - \omega_n)^2}, \end{aligned} \quad (42)$$

where $\xi_{\pm}(k, n) = \sum_{l=n+1}^{k-1} (\omega_l - \omega'_l \pm \bar{\omega}_l/2)$.

We shall now explore several applications and limiting cases of these results. We start by considering the second-order rate [Eq. (34)]. Combining Eqs. (37) and (38), we have

$$\begin{aligned} W_{mn}^{(2)}(s) &= \left(\frac{v_{mn}}{\hbar}\right)^2 \int_0^{\infty} ds e^{-st} \int_0^t d\tau \int_0^t d\tau' \\ &\times \sigma_m(\tau - \tau') \sigma'_n(\tau' - \tau). \end{aligned} \quad (43)$$

Using the properties of the Laplace transform, this gives the rate that depends on the normalized absorption and fluorescence spectra of the two sites:

$$\begin{aligned} K_{mn}^{(2)}(s) &= 2\pi \left(\frac{v_{mn}}{\hbar}\right)^2 \int_{-\infty}^{\infty} \frac{d\omega_m d\omega_n}{2\pi} \sigma_m(\omega_m) \\ &\times \sigma'_n(\omega_n) \frac{s/\pi}{s^2 + (\omega_m - \omega_n)^2}. \end{aligned} \quad (44)$$

Setting $s=0$, we can use the relation

$$\lim_{s \rightarrow 0} \frac{s/\pi}{x^2 + s^2} = \delta(x), \quad (45)$$

and recover Förster's rate,⁵¹

$$K_{mn}^{(2)} = 2\pi \left(\frac{v_{mn}}{\hbar}\right)^2 \int_{-\infty}^{\infty} \frac{d\omega}{2\pi} \sigma_m(\omega) \sigma'_n(\omega). \quad (46)$$

In the static limit, $\kappa_n \ll 1$, we have

$$\sigma_n(t) = \exp\left[-i\Omega_{n,g}t - \frac{\Delta_n^2}{2}t^2\right] \quad (47)$$

and

$$\sigma'_n(t) = \exp\left[-i\Omega_{n,e}t - \frac{\Delta_n^2}{2}t^2\right], \quad (48)$$

with $\Omega_{n,g} = \Omega_n + \lambda_n$ and $\Omega_{n,e} = \Omega_n - \lambda_n$. The absorption and fluorescence lineshapes assume in this case the Gaussian profiles,

$$\sigma_n(\omega) = \left(\frac{h}{2k_B T \lambda_n}\right)^{1/2} \exp\left\{-\frac{\hbar(\omega - \Omega_{n,g})^2}{4k_B T \lambda_n}\right\}, \quad (49)$$

and $\sigma'_n(\omega) = \sigma_n(\omega + 2\lambda_n)$, i.e. the fluorescence maximum is shifted by $2\lambda_n$ (the Stokes shift) to the red relative to the absorption. The Förster rate now becomes

$$K_{mn}^{(2)} = \left(\frac{v_{mn}}{\hbar}\right)^2 \left(\frac{h}{4k_B T(\lambda_n + \lambda_m)}\right)^{1/2} \times \exp\left\{-\frac{\hbar(\Omega_{n,e} - \Omega_{m,g})^2}{4k_B T(\lambda_n + \lambda_m)}\right\}. \quad (50)$$

The sequential transfer limit applies if we can identify a single path where only the fluorescence spectrum of the n th molecule and the absorption spectrum of the $(n+1)$ th molecule overlap. We further assume that subsequent transfer events are uncorrelated and the four-point correlation functions factorize into products of two-point correlation functions,

$$\Gamma_n(t_1, t_2, t_3, t_4) = \sigma_n(t_1 - t_4) \sigma'_n(t_3 - t_2). \quad (51)$$

For this case, the DA transfer is completely described in terms of nearest neighbor second-order rates $K_{n+1,n}^{(2)}(s)$ given in Eq. (44). All higher-order terms are canceled by the second term in Eq. (36) as a consequence of the factorization (51). This will be demonstrated for a three-site in Sec. V.

If the intramolecular relaxation is fast compared to the transfer time, $\hbar\Lambda_n \gg v_{n,n+1}$, the function F_n in Eq. (17) takes the form

$$F_n(t_1, t_2, t_3, t_4) = \frac{\Delta_n^2}{2}(t_1 - t_4)^2 + \frac{\Delta_n^2}{2}(t_3 - t_2)^2 - 2i\lambda_n(t_3 - t_2), \quad (52)$$

and the factorization (51) becomes exact with the rate given by Eq. (50).

We next assume that only the acceptor's absorption and the donor's fluorescence spectra overlap, while all the intermediate bridge molecules ($n = 2, \dots, m-1$) have higher energies. For this limit the populations of the bridge molecules are negligible at all times, and the Förster nearest neighbor rate equation cannot be used to describe the transfer process. Using the superexchange model,^{10,11,52} we expect these bridge states to modify the effective DA coupling.

Since in the super-exchange limit the bridge molecules are excited only virtually for a very short time, we can calculate the four-point correlation function in the short time limit, $\Lambda_n t \ll 1$,

$$\begin{aligned} \Gamma_k(t_k, t_{k+1}, t'_{k+1}, t'_k) &= \exp\left\{-i\Omega_{k,g}(t_k - t_{k+1} + t'_{k+1} - t'_k) \right. \\ &\quad \left. - \frac{\Delta_k^2}{2}(t_k - t_{k+1} + t'_{k+1} - t'_k)^2\right\}, \end{aligned} \quad (53)$$

for $k = n+1, \dots, m-1$. Using the Fourier transform of Gaussian functions,

$$\exp\left\{-\frac{\Delta_k^2}{2}t^2\right\} = \left(\frac{2\pi}{\Delta_k^2}\right)^{1/2} \int_{-\infty}^{\infty} \frac{d\omega}{2\pi} \exp\left\{-\frac{\omega^2}{2\Delta_k^2} - i\omega t\right\}, \quad (54)$$

one obtains for the bridge spectral function

$$\begin{aligned} S_{mn}(\omega_m, \omega_n; s) &= 2\pi \frac{s/\pi}{s^2 + (\omega_m - \omega_n)^2} \\ &\times \left[\prod_{k=n+1}^{m-1} \int_{-\infty}^{\infty} \frac{d\omega_k}{2\pi} \frac{1}{(\omega_k - \omega_n)^2} \right. \\ &\quad \left. \times \left(\frac{2\pi}{\Delta_k^2}\right)^{1/2} \exp\left\{-\frac{(\omega_k - \Omega_{k,g})^2}{2\Delta_k^2}\right\} \right]. \end{aligned} \quad (55)$$

In order to study the transfer via virtual intermediate states, we assume that the energy gap between the donor and any bridge molecule is much larger than the characteristic widths, Δ_n . This enables us to calculate the frequency integrals in Eq. (55) to get

$$\begin{aligned} &\left[\prod_{k=n+1}^m \left(\frac{v_{k,k-1}}{\hbar}\right)^2 \right] S_{mn}(\omega_m, \omega_n; s) \\ &= 2\pi |V_{\text{eff}}|^2 \frac{s/\pi}{s^2 + (\omega_m - \omega_n)^2}, \end{aligned} \quad (56)$$

with

$$V_{\text{eff}} = \frac{v_{n+1,n}}{\hbar} \prod_{k=n+1}^{m-1} \frac{v_{k+1,k}/\hbar}{\Omega_{n,e} - \Omega_{k,g}}. \quad (57)$$

Comparison with Eq. (44) shows that the DA rate is equivalent to the rate for sequential transfer between neighboring sites, with the intermolecular coupling replaced by an effective DA coupling V_{eff} . In this limit, which agrees with the conventional treatment of the superexchange problem (see, e.g., Refs. 10 and 52), the bridge only provides an effective intermolecular coupling constant that enters the rate as a prefactor. From Eq. (42) it is evident, however, that the influence of the bridge is generally more complex and its entire spectral properties need to be taken into account.

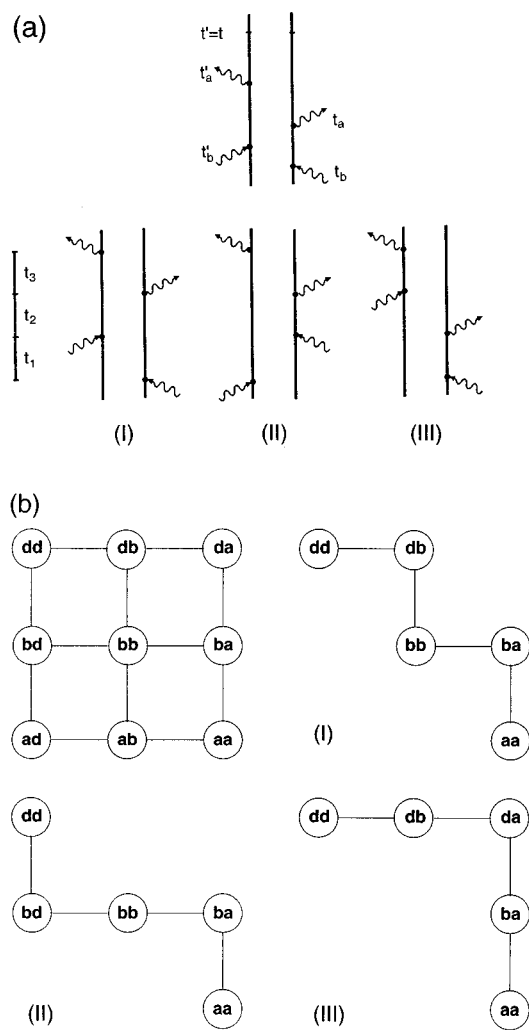


FIG. 5. The Feynman diagram corresponding to Eq. (59), in which the bra and the ket are not mutually time ordered, is shown (top), together with the diagrams that result after time ordering (bottom) [panel (a)]. The latter can be associated with distinct Liouville space pathways for energy transfer in the three-site system [panel (b)]. The contributions to the DA transfer rate in Eq. (61) are due to the population paths (I) and (II), as well as the coherence path (III) and their complex conjugates.

V. SEQUENTIAL VERSUS SUPEREXCHANGE TRANSFER IN A THREE-SITE SYSTEM

The primary charge transfer in the RC of photosynthetic bacteria is usually described using a three-site system (The donor is a bacteriochlorophyll dimer called the special pair, the acceptor is a bacteriopeophytin molecule, whereas an accessory bacteriochlorophyll may act as a bridge.¹⁴) Considerable efforts have been devoted to clarify the role of the bridge for the efficient and fast (3 ps at room temperature^{13,15,16}) charge separation. In particular, it has been shown that the vibrational dephasing time scale is likely to be comparable to the transfer time, which renders the conventional Förster theory inapplicable.¹⁶ Liouville space analysis in the static limit,¹¹ and the real time path integral techniques,¹⁵ have been applied to this problem. In the following we will carry out a complete analysis of all limiting

cases of a general three-site system with an arbitrary time scale for nuclear motion. The rates will be calculated to lowest nonvanishing order in intermolecular coupling. This applies to typical biological systems, where electronic dephasing (i.e., the absorption linewidth) is larger ($\approx 400 \text{ cm}^{-1}$) than the intermolecular coupling ($\approx 40 \text{ cm}^{-1}$). Using Eq. (36), the DA energy transfer rate is

$$K_{ad}^{(4)}(s) = s^2 W_{ad}^{(4)}(s) - s^3 W_{ab}^{(2)}(s) W_{bd}^{(2)}(s), \quad (58)$$

where $W_{mn}^{(2)}(s)$ is given by Eq. (43) and

$$W_{ad}^{(4)}(s) = \left(\frac{v_{ab} v_{db}}{\hbar^2} \right)^2 \int_0^\infty dt e^{-st} \times \int_0^t dt_a \int_{-\infty}^{t_a} dt_b \int_0^t dt'_a \int_{-\infty}^{t'_a} dt'_b \times \sigma_a(t_a - t'_a) \Gamma_b(t_b, t_a, t'_a, t'_b) \sigma'_d(t'_b - t_b). \quad (59)$$

We shall express the rate by means of the Liouville space formulation of quantum dynamics, as used in the treatment of the nonlinear optical response.⁴³ This amounts to changing the time variables in the above integrations and breaking the rhs of Eq. (59) into several contributions with all possible time orderings [see Fig. 5(a)]. As shown in Ref. 11 the rate can be expressed in terms of correlation functions that represent the different Liouville space pathways for energy transfer (see Fig. 5),

$$K_{mn}^{(2)}(s) = 2 \left(\frac{v_{mn}}{\hbar} \right)^2 \text{Re} \langle \mathcal{S}_{nm}(s) \rangle, \quad (60)$$

$$K_{ad}^{(4)}(s) = 2 \left(\frac{v_{ab} v_{db}}{\hbar^2} \right)^2 \text{Re} \left\{ \left[\langle \mathcal{S}_{ba}(s) \mathcal{S}_{bb}(s) \mathcal{S}_{db}(s) \rangle - \frac{1}{s} \langle \mathcal{S}_{ba}(s) \rangle \langle \mathcal{S}_{db}(s) \rangle \right] + \left[\langle \mathcal{S}_{ba}(s) \mathcal{S}_{bb}(s) \mathcal{S}_{ba}(s) \rangle - \frac{1}{s} \langle \mathcal{S}_{ba}(s) \rangle \langle \mathcal{S}_{bd}(s) \rangle \right] + \langle \mathcal{S}_{ba}(s) \mathcal{S}_{da}(s) \mathcal{S}_{db}(s) \rangle \right\}. \quad (61)$$

Here we introduced the frequency domain Green's functions $\mathcal{S}_{mn}(s)$, defined by its action on an arbitrary Hilbert space operator A ,

$$\mathcal{S}_{mn}(s) A = \int_0^\infty dt e^{-st} e^{-iH_m t/\hbar} A e^{iH_n t/\hbar}. \quad (62)$$

The first two terms in Eq. (61) represent sequential contributions to the rate, since they involve a population of the bridge state (Fig. 5, paths I and II) (The subtraction of the respective uncorrelated expressions results in a cancellation of the $1/s$ singularity, as will be shown shortly.) The third

term represents energy transfer via a virtual bridge state, which constitutes the superexchange component (Fig. 5, path III).

In Appendix A we derive closed expressions for the rates in (60) and (61). For the donor–bridge transfer rate we get

$$K_{bd}^{(2)}(s) = -2 \left(\frac{v_{bd}}{\hbar} \right)^2 \operatorname{Im} \sum_{m=0}^{\infty} \frac{(-z_d)^m}{m!} \times e^{z_d} J_0 \left(s + m\Lambda_d + \frac{\hat{\Gamma}_d}{2}, \Omega_d - \Omega_{b,g} \right), \quad (63)$$

and for the DA rate we obtain

$$K_{ad}^{(4)}(s) = 2 \left(\frac{v_{ab}v_{db}}{\hbar^2} \right)^2 \operatorname{Re} \sum_{n=1}^{\infty} \sum_{m,p=0}^{\infty} \frac{(-z_a^*)^m}{n!m!p!} e^{z_a^*} \left\{ (-z_b)^n (-z_d)^p e^{z_d} \times \frac{J_n^*(s + m\Lambda_a + \hat{\Gamma}_a/2, \Omega_{b,e} - \Omega_a) \tilde{J}_n(s + p\Lambda_d + \hat{\Gamma}_d/2, \Omega_d - \Omega_{b,g})}{s + n\Lambda_b} - (z_b^*)^n (-z_d^*)^p e^{z_d^*} \times \frac{J_n^*(s + m\Lambda_a + \hat{\Gamma}_a/2, \Omega_{b,e} - \Omega_a) \tilde{J}_n^*(s + p\Lambda_d + \hat{\Gamma}_d/2, \Omega_d - \Omega_{b,g})}{s + n\Lambda_b} + (z_b^*)^n (-z_d^*)^p e^{z_d^*} \times \frac{J_n(s + m\Lambda_a + \hat{\Gamma}_a/2, \Omega_a - \Omega_{b,g}) J_n^*(s + p\Lambda_d + \hat{\Gamma}_d/2, \Omega_d - \Omega_{b,g})}{s + n\Lambda_b + m\Lambda_a + p\Lambda_d + (\hat{\Gamma}_d + \hat{\Gamma}_a)/2 + i(\Omega_d - \Omega_a)} \right\}. \quad (64)$$

Here $z_n = (\hat{\Gamma}_n/2 - i\lambda_n)/\Lambda_n$, $\hat{\Gamma}_n = 2\Delta_n^2/\Lambda_n$, and we have introduced the auxiliary functions,

$$J_n(s, \Omega) = -i \int_0^{\infty} dt e^{-st} e^{i\Omega t - g_b(t)} (1 - e^{-\Lambda_b t})^n \quad (65)$$

and

$$\tilde{J}_n(s, \Omega) = -i \int_0^{\infty} dt e^{-st} e^{i\Omega t - g_b(t)} \left(\frac{z_b^*}{z_b} - e^{-\Lambda_b t} \right)^n. \quad (66)$$

A practical numerical procedure for evaluating the integrals in Eqs. (65) and (66) is to express them in terms of confluent hypergeometric functions,^{43,53} which can then be calculated using recursion relations.

Equations (63) and (64) hold for an arbitrary solvent time scale. In the static limit they reproduce the results of

Ref. 11. The homogeneous limit of fast nuclear motion can be obtained from (63) and (64) by retaining only the first term in the summations over n , m , and p . As the solvent time scale slows down (Λ decreases), we need to keep more terms in the summation since the sum converges more slowly. In the static limit, $\Lambda \rightarrow 0$, we can still use these expressions. However, in this case it is more convenient to evaluate the necessary integrals directly. Following Refs. 11 and 44 we write $K_{ad}^{(4)}(s) = K_{ad}^{(4),p}(s) + K_{ad}^{(4),c}(s)$, where the resulting contribution due to the population pathways is

$$K_{ad}^{(4),p}(s) = \left(\frac{v_{ab}v_{db}}{\hbar^2} \right)^2 (2\pi)^2 \int_0^{\infty} dt e^{-st} \int_{-\infty}^{\infty} dx dy \times \frac{s/\pi}{s^2 + x^2} \frac{s/\pi}{s^2 + y^2} [W(x, t; y) - W(x, \infty; y)], \quad (67)$$

with $(\Delta_{mn}^2 = \Delta_m^2 + \Delta_n^2)$

$$W(x, t; y) = \frac{1}{2\pi [\Delta_{ab}^2 \Delta_{bd}^2 - \Delta_b^4 M_b^2(t)]^{1/2}} \exp \left\{ - \frac{\Delta_{ab}^2 (y - (\Omega_{d,e} - \Omega_{b,g}))^2 + \Delta_{bd}^2 (x - (\Omega_{b,g}(t) - \Omega_{a,g}))^2}{2[\Delta_{ab}^2 \Delta_{bd}^2 - \Delta_b^4 M_b^2(t)]} \right\} \times \exp \left\{ - \frac{2\Delta_b^2 M_b(t) [(y - (\Omega_{d,e} - \Omega_{b,g})) (x - (\Omega_{b,g}(t) - \Omega_{a,g}))]}{2[\Delta_{ab}^2 \Delta_{bd}^2 - \Delta_b^4 M_b^2(t)]} \right\}. \quad (68)$$

Here $W(x,t;y)$ is the conditional probability for the electronic gap coordinate $U = H_0 - H_{\text{nuc}} - \langle H_0 - H_{\text{nuc}} \rangle$ to attain the value x at time t given that it started at y at $t=0$. We further introduced the relaxation function,

$$M_b(t) = \langle e^{iH_{\text{nuc}}t} U_b e^{-iH_{\text{nuc}}t} U_b \rangle / \Delta_b^2, \quad (69)$$

where $U_b = H_b - \hbar \Omega_{b,g}$ is the electronic gap coordinate for the bridge, and

$$\Omega_{b,g}(t) = \Omega_{b,g} + \langle \exp(iH_b t) U_b \times \exp(-iH_b t) \rangle$$

For the coherence (superexchange) pathway, we obtain

$$K_{ad}^{(4),c}(s) = \left(\frac{v_{ab} v_{db}}{\hbar^2} \right)^2 \int_{-\infty}^{\infty} dz \frac{s/\pi}{s^2 + z^2} [I_{de,ag}(z,s) - I_{bg,ag}(z,s) - I_{de,bg}(z,s)], \quad (70)$$

where

$$I_{kp,jq}(z,s) = - \frac{2\pi}{\sqrt{4\pi k_B T (\lambda_k + \lambda_j)}} e^{-(z - (\Omega_{k,p} - \Omega_{j,q}))^2 / 4k_B T (\lambda_k + \lambda_j)} \int_0^{\infty} dx \frac{\sin(zx/2)}{z/2} \cos \left\{ \left[\left(\frac{1}{2} - \frac{\lambda_b}{\lambda_k + \lambda_j} \right) z + \frac{\lambda_k (\Omega_{d,e} - \Omega_{j,q}) + \lambda_j (\Omega_{d,e} - \Omega_{k,p})}{\lambda_k + \lambda_j} \right] x \right\} \exp \left(-sx - \frac{x^2}{2R_{kj}} \right), \quad (71)$$

with

$$R_{kj}^{-1} = 2k_B T \left[\frac{(\lambda_b + \lambda_d)(\lambda_a + \lambda_b) - \lambda_b^2}{\lambda_k + \lambda_j} \right]. \quad (72)$$

A Padé approximation for the integral in Eq. (71) in the zero-frequency ($s=0$) limit has been derived [Eq. (4.21) of Ref. 11].

In Figs. 6–10 we display the frequency-dependent rates $K_{bd}^{(2)}(s)$ and $K_{ad}^{(4)}(s)$ calculated using Eqs. (63) and (64) for different electronic state energies. In all calculations the FWHM of the linear absorption spectrum and the Stokes shift parameter is held fixed ($\hbar \Gamma_n = 0.025$ eV, $\hbar \lambda_n = 0.005$ eV). The intermolecular coupling is $v_{ab} = v_{db} = 0.01$ eV. The parameter $\kappa_n = \Lambda_n / \sqrt{2\lambda_n k_B T / \hbar}$ [Eq. (22)], which denotes the ratio of a typical nuclear frequency to the static linewidth, was varied by changing the temperature.

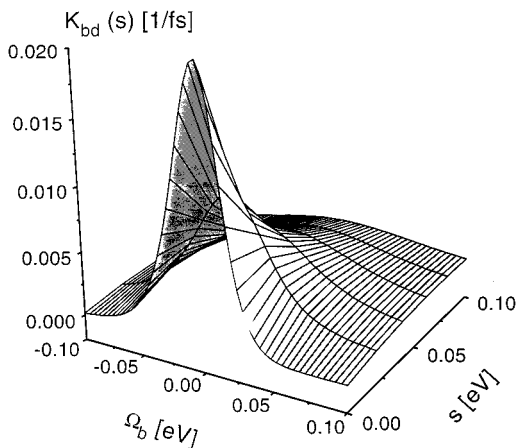


FIG. 6. Frequency-dependent donor-bridge transfer rate [Eq. (63)] as a function of the bridge energy ($\Omega_d=0$ for $\kappa_n=1.0$ ($T=319$ K)). The other parameters are $\hbar \Gamma_n=0.025$ eV and $\hbar \lambda_n=0.005$ eV, and $v_{bd}=0.01$ eV.

In Fig. 6 we show the dependence of $K_{bd}^{(2)}(s)$ on the bridge energy Ω_b ($\Omega_d=0.0$) for $\kappa_n=1.0$ ($T=319$ K). The rate shows a pronounced maximum when the bridge energy is close to resonance with Ω_d . The exact position of this maximum depends on the nuclear motion time scale. If $\kappa_n \gg 1$ (homogeneous limit) the maximum is at $\Omega_b = \Omega_d$. In the static limit ($\kappa_n \ll 1$), however, the transfer is most favored when the bridge energy is detuned from Ω_d to compensate for the Stokes shift, i.e., $\Omega_b = \Omega_{d,e} - \lambda_b$. This agrees with the behavior of spectral lineshapes. The Stokes shift observed in the static limit disappears in the homogeneous (motional narrowing) limit.

Next we focus on a three-site system. In Fig. 7 we show the dependence of $K_{ad}^{(4)}(s)$ on the bridge energy Ω_b . The donor and the acceptor energies are equal ($\Omega_d = \Omega_a = 0.0$) and $\kappa_n = 1.0$ ($T = 319$ K). The rate has a maximum when the bridge energy passes through the region of the DA electronic states. The influence of the nuclear dynamics time scale on the zero frequency rate is shown in Fig. 8, for $\kappa_n = 0.5$ ($T = 187$ K) and $\kappa_n = 1.25$ ($T = 413$ K). Obviously, an increase of κ_n causes an overall reduction of the rate and a shift in the resonance positions. Moreover, the rate shows a weaker dispersion. As in Fig. 6 the homogeneous limit yields a maximum rate if all energy levels are degenerated, while in the inhomogeneous limit the Stokes shift has to be compensated for optimal transfer. It has been shown¹¹ that for a detuning between the donor and the acceptor energy that exceeds the linewidth, the rate $K_{ad}^{(4)}(s)$ can become negative for small values of s . The same holds for the arbitrary nuclear dynamics time scale considered here. In Figs. 9 and 10 we plot the DA rate when the donor and acceptor energies are detuned by Γ_n . The calculated rate becomes negative if the bridge state passes the resonance with the donor state, whereas it is positive for the resonance with the acceptor state. This behavior is insensitive to a variation of κ_n , as can be seen in Fig. 10. For large s the rate is always positive. The negative

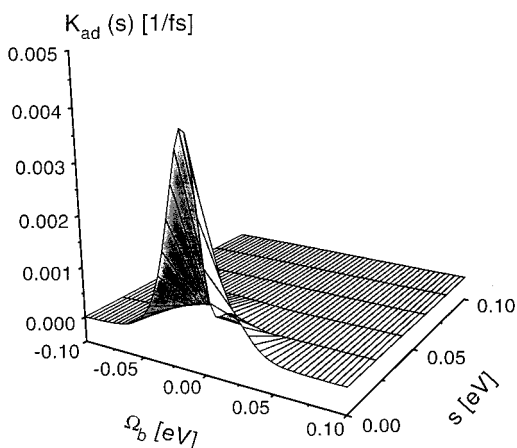


FIG. 7. Frequency-dependent DA-transfer rate [Eq. (64)] as a function of the bridge energy. $\Omega_d = \Omega_a = 0$ and $v_{bd} = v_{ab} = 0.01$ eV. Other parameters are as in Fig. 6.

values for the frequency-dependent rate indicate a breakdown of the Markov approximation, as pointed out in Ref. 11. The solution of the ordinary rate equations leads to negative occupation probabilities in the short time dynamics, and the use of the generalized rate equations that contain the full frequency dependence of $K_{mn}^{(4)}(s)$ becomes essential.

VI. SUMMARY

The present correlation function approach for the excitation and electron dynamics in molecular aggregates provides a powerful tool for studying optical and transport properties of these systems. This has been shown first by calculating time- and frequency-resolved fluorescence spectra for an aggregate with five monomers. This example demonstrates the capabilities of the present approach, which can easily be extended to larger aggregates with more than one nuclear mode per monomer. In a three-dimensional system like the light harvesting complex of green plants,¹⁹ for instance, a simulation of energy transfer between the most blue and the most

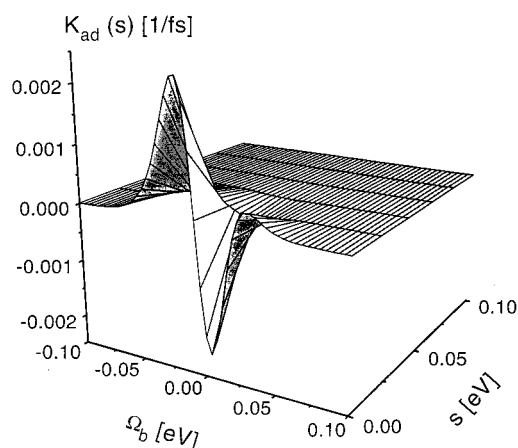


FIG. 9. Frequency-dependent DA-transfer rate [Eq. (64)] as a function of the bridge energy if $\Omega_d - \Omega_a = \Gamma_n$ for $\kappa_n = 1.0$ ($T = 319$ K). Other parameters are as in Fig. 7.

red pigments²⁰ would require a summation over all possible pathways connecting these monomers. In practice, however, only a few pathways are expected to give relevant contributions to the signal. Hence, even though the perturbative treatment restricts the iterative procedure to the short time dynamics, it has some clear advantages compared with the derivation of a master equation that treats the vibronic levels explicitly and is restricted to small systems. The incorporation of coherent effects such as quantum beats¹⁶ as well as the treatment of other nonlinear spectroscopies (e.g., photon echo²⁷ and hole burning²⁵) can be readily accomplished using the present approach.

The characterization of long-range energy and charge transfer processes using frequency-dependent rates is a major focus of theoretical and experimental interest. Starting with the two-point correlation function for exciton operators, we have given general formulas for the rate in the sequential and the superexchange limit, which hold in lowest-order perturbation theory with respect to the intermolecular coupling.

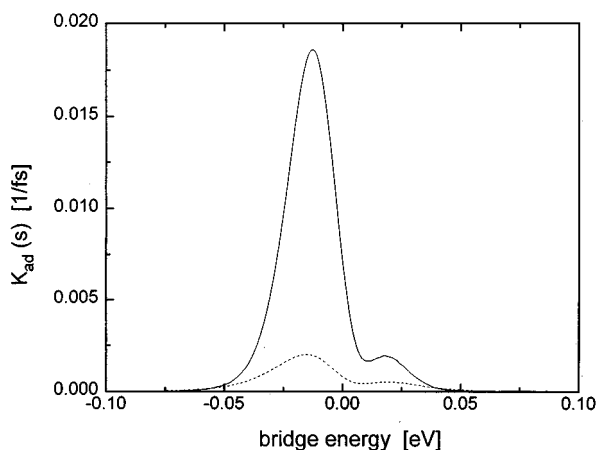


FIG. 8. Zero-frequency DA-transfer rate [Eq. (64)] as a function of the bridge energy if $\Omega_d = \Omega_a = 0$ for $\kappa_n = 0.5$ ($T = 187$ K) (solid) and $\kappa_n = 1.25$ ($T = 413$ K) (dashed). Other parameters are the same as in Fig. 7.

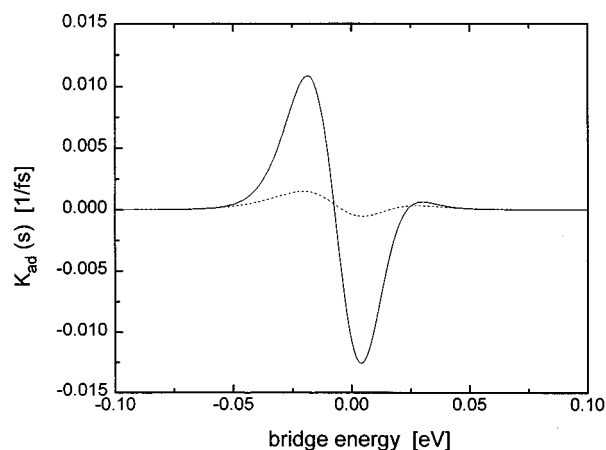


FIG. 10. Zero-frequency DA-transfer [Eq. (64)] rate as a function of the bridge energy if $\Omega_d - \Omega_a = \Gamma_n$ for $\kappa_n = 0.5$ ($T = 187$ K) (solid) and $\kappa_n = 1.25$ ($T = 413$ K) (dashed). The other parameters are the same as in Fig. 7.

Our expressions show how the bridge influences the DA transfer through its spectral properties. Finally, Liouville space Green's functions have been used to derive analytical expressions for the rate matrix in a three-site system, which hold for an arbitrary time scale of the nuclear motion. These calculations should allow the interpretation of optical measurements conducted on the photosynthetic reaction center. Our numerical examples illustrate the influence of the various parameters characterizing the electronic structure, as well as the dynamics of the nuclear degrees of freedom.

ACKNOWLEDGMENTS

This work was supported by the National Science Foundation and the Air Force Office of Scientific Research. O.K. gratefully acknowledges a postdoctoral fellowship from the German Academic Exchange Service (DAAD).

APPENDIX: DERIVATION OF THE THREE-SITE TRANSFER RATES

The derivation of Eqs. (63) and (64) follows the procedure used in the calculation of fluorescence and Raman spectroscopy of two level systems (Chaps. 8 and 9 of Ref. 43). To this end we first write the rhs of Eqs. (60) and (61) in terms of multiple time integrals,

$$K_{mn}^{(2)}(s) = 2 \left(\frac{v_{mn}}{\hbar} \right)^2 \operatorname{Re} \int_0^\infty dt e^{-st} \langle \mathcal{S}_{nm}(t) \rangle, \quad (\text{A1})$$

and

$$\begin{aligned} K_{ad}^{(4)}(s) = & 2 \left(\frac{v_{ab} v_{db}}{\hbar^2} \right)^2 \operatorname{Re} \int_0^\infty \int_0^\infty \int_0^\infty dt_1 dt_2 dt_3 \\ & \times e^{-s(t_1+t_2+t_3)} \{ [\langle \mathcal{S}_{ba}(t_3) \mathcal{S}_{bb}(t_2) \mathcal{S}_{db}(t_1) \rangle \\ & - \langle \mathcal{S}_{ba}(t_3) \rangle \langle \mathcal{S}_{db}(t_1) \rangle] \\ & + [\langle \mathcal{S}_{ba}(t_3) \mathcal{S}_{bb}(t_2) \mathcal{S}_{bd}(t_1) \rangle - \langle \mathcal{S}_{ba}(t_3) \rangle \\ & \times \langle \mathcal{S}_{bd}(t_1) \rangle] + \langle \mathcal{S}_{ba}(t_1) \mathcal{S}_{da}(t_2) \mathcal{S}_{db}(t_3) \rangle \}. \end{aligned} \quad (\text{A2})$$

Using the correlation functions that have been introduced in the treatment of the nonlinear optical response of two-level systems,⁴³ we find

$$K_{mn}^{(2)}(s) = 2 \left(\frac{v_{mn}}{\hbar} \right)^2 \operatorname{Re} \int_0^\infty dt e^{-st} J_{m,g}(t) J_{n,e}^*(t), \quad (\text{A3})$$

and

$$\begin{aligned} K_{ad}^{(4)}(s) = & 2 \left(\frac{v_{ab} v_{db}}{\hbar^2} \right)^2 \operatorname{Re} \int_0^\infty \int_0^\infty \int_0^\infty dt_1 dt_2 dt_3 \\ & \times e^{-s(t_1+t_2+t_3)} \{ J_{a,g}^*(t_1) [R_1^b(t_1, t_2, t_3) \\ & - J_{b,e}(t_1) J_{b,g}(t_3)] J_{d,e}^*(t_3) + J_{a,g}^*(t_1) \\ & \times [R_2^b(t_1, t_2, t_3) - J_{b,e}(t_1) J_{b,g}^*(t_3)] J_{d,e}(t_3) \\ & + J_{a,g}^*(t_1+t_2) R_3^b(t_1, t_2, t_3) J_{d,e}(t_2+t_3) \}, \end{aligned} \quad (\text{A4})$$

where we have introduced the time domain response functions,

$$\begin{aligned} J_{m,g}(t) &= \exp(-i\Omega_{m,g}t - g_m(t)), \\ J_{m,e}(t) &= \exp(-i\Omega_{m,e}t - g_m^*(t)), \\ R_1^b(t_1, t_2, t_3) &= \exp(-i\Omega_{b,g}t_1 - i\Omega_{b,g}t_3 - g_b^*(t_1) - g_b(t_3) \\ &\quad - f_b^{(+)}(t_1, t_2, t_3)), \quad (\text{A5}) \\ R_2^b(t_1, t_2, t_3) &= \exp(-i\Omega_{b,g}t_1 + i\Omega_{b,g}t_3 - g_b^*(t_1) \\ &\quad - g_b^*(t_3) + f_b^{(+)*}(t_1, t_2, t_3)), \\ R_3^b(t_1, t_2, t_3) &= \exp(-i\Omega_{b,g}t_1 + i\Omega_{b,g}t_3 - g_b(t_1) - g_b^*(t_3) \\ &\quad + f_b^{(-)*}(t_1, t_2, t_3)), \end{aligned}$$

with the auxiliary functions

$$\begin{aligned} f_b^{(+)}(t_1, t_2, t_3) &= g_b(t_2) - g_b(t_1+t_2) - g_b(t_2+t_3) \\ &\quad + g_b(t_1+t_2+t_3), \\ f_b^{(-)}(t_1, t_2, t_3) &= g_b^*(t_2) - g_b^*(t_1+t_2) - g_b(t_2+t_3) \\ &\quad + g_b(t_1+t_2+t_3). \end{aligned} \quad (\text{A6})$$

Using the overdamped Brownian oscillator model [Eqs. (21) and (22)], the auxiliary functions f_b can be rewritten as

$$\begin{aligned} f_b^{(+)}(t_1, t_2, t_3) &= -2i\lambda_b t_1 + z_b e^{-\Lambda_b t_2} (1 - e^{-\Lambda_b t_1}) \\ &\quad \times (z_b^*/z_b - e^{-\Lambda_b t_3}), \\ f_b^{(-)}(t_1, t_2, t_3) &= z_b e^{-\Lambda_b t_2} (1 - e^{-\Lambda_b t_1}) (1 - e^{-\Lambda_b t_3}). \end{aligned} \quad (\text{A7})$$

A Taylor expansion of the exponent yields, for the correlation functions,

$$\begin{aligned} R_1^b(t_1, t_2, t_3) &= J_{b,e}(t_1) J_{b,g}(t_3) \sum_{n=0}^{\infty} \frac{(-z_b)^n}{n!} e^{-\Lambda_b n t_2} \\ &\quad \times (1 - e^{-\Lambda_b t_1})^n \left(\frac{z_b^*}{z_b} - e^{-\Lambda_b t_3} \right)^n, \\ R_2^b(t_1, t_2, t_3) &= J_{b,e}(t_1) J_{b,g}^*(t_3) \sum_{n=0}^{\infty} \frac{(z_b^*)^n}{n!} e^{-\Lambda_b n t_2} \\ &\quad \times (1 - e^{-\Lambda_b t_1})^n \left(\frac{z_b}{z_b^*} - e^{-\Lambda_b t_3} \right)^n, \quad (\text{A8}) \\ R_3^b(t_1, t_2, t_3) &= J_{b,g}(t_1) J_{b,g}^*(t_3) \sum_{n=0}^{\infty} \frac{(z_b^*)^n}{n!} e^{-\Lambda_b n t_2} \\ &\quad \times (1 - e^{-\Lambda_b t_1})^n (1 - e^{-\Lambda_b t_3})^n. \end{aligned}$$

Comparing Eqs. (60) and (A8) we note the cancellation of the $1/s$ singularity by the $n=0$ term. Thus, when substituted in Eq. (60) the sum will start at $n=1$. We shall express the rate in terms of the functions $J_n(s, \Omega)$ and $\tilde{J}_n(s, \Omega)$ defined in Eqs. (65) and (66), which refer to the bridge. We thus use the following expansion for the time domain response functions related to the donor or the acceptor,

$$J_{m,g}(t) = e^{-i\Omega_m t - \hat{\Gamma}_m t/2} e^{z_m} \sum_{p=0}^{\infty} \frac{(-z_m)^p}{p!} e^{-\Lambda_m p t} \quad (\text{A9})$$

and

$$J_{m,e}(t) = e^{-i\Omega_m t - \hat{\Gamma}_m t/2} e^{z_m^*} \sum_{p=0}^{\infty} \frac{(-z_m^*)^p}{p!} e^{-\Lambda_m p t}. \quad (\text{A10})$$

Combining Eqs. (A8)–(A10) with Eqs. (65) and (66) gives the bd rate [Eq. (63)] as well as the ad rate [Eq. (64)].

- ¹M. A. Fox and M. Chanon, in *Photoinduced Electron Transfer* (Elsevier, Amsterdam, 1989).
- ²N. Mataga, T. Okada, and H. Masukara, in *Dynamics and Mechanics of Photoinduced Electron Transfer and Related Phenomena* (North-Holland, Amsterdam, 1992).
- ³D. R. Casimiro, L. L. Wong, J. L. Colon, T. E. Zewert, J. H. Richards, I. J. Chang, J. R. Winkler, and H. B. Gray, *J. Am. Chem. Soc.* **115**, 1485 (1993).
- ⁴R. van Grondelle, J. P. Dekker, T. Gillbro, and V. Sundstrom, *Biochim. Biophys. Acta* **1187**, 1 (1994).
- ⁵C. J. Murphy, M. R. Arkin, Y. Jenkins, N. D. Ghatlia, S. H. Bossmann, N. J. Turro, and J. K. Barton, *Science* **262**, 1025 (1993); J. Murphy, M. R. Arkin, N. D. Ghatlia, S. H. Bossmann, N. J. Turro, and J. K. Barton, *Proc. Natl. Acad. Sci. USA* **91**, 5315 (1994).
- ⁶S. M. Risser, D. N. Beratran, and T. M. Meade, *J. Am. Chem. Soc.* **115**, 2508 (1993).
- ⁷J. M. Gruschus and A. Kuki, *J. Phys. Chem.* **97**, 5581 (1993).
- ⁸S. Speiser, *Chem. Rev.* (in press).
- ⁹J. N. Onuchic and D. N. Beratran, *J. Chem. Phys.* **92**, 722 (1990).
- ¹⁰R. A. Marcus, *Chem. Phys. Lett.* **133**, 471 (1987).
- ¹¹Y. Hu and S. Mukamel, *J. Chem. Phys.* **91**, 6973 (1989).
- ¹²M. Bixon, J. Jortner, and M. E. Michel-Beyerle, *Biochim. Biophys. Acta* **1056**, 301 (1991).
- ¹³M. Marchi, J. N. Gehlen, D. Chandler, and M. Newton, *J. Am. Chem. Soc.* **115**, 4178 (1993).
- ¹⁴G. R. Fleming and R. van Grondelle, *Phys. Today* **47**, 48 (1994).
- ¹⁵R. Egger and C. H. Mak, *J. Phys. Chem.* **98**, 9903 (1994).
- ¹⁶M. H. Vos, M. R. Jones, C. N. Hunter, J. Breton, and J. L. Martin, *Proc. Natl. Acad. Sci. USA* **91**, 12 701 (1994).
- ¹⁷A. K. Felts, W. T. Pollard, and R. A. Friesner, *J. Chem. Phys.* **99**, 2929 (1995).
- ¹⁸G. McDermott, S. M. Prince, A. A. Freer, A. M. Hawthornthwaite-Lawless, M. Z. Papiz, R. J. Cogdell, and N. W. Isaacs, *Nature* **374**, 517 (1995).
- ¹⁹W. Kühlbrandt, D. N. Wang, and Y. Fujitoshi, *Nature* **367**, 614 (1994).
- ²⁰T. Bittner, G. P. Wiederrecht, K. D. Irrgang, G. Renger, and M. R. Wasielewski, *Chem. Phys.* **194**, 311 (1995).
- ²¹V. M. Agranovich and M. D. Galanin, *Electronic Excitation Energy Transfer in Condensed Matter* (North-Holland, Amsterdam, 1982).
- ²²V. Cernyak, N. Wang, and S. Mukamel, *Phys. Rep.* **263**, 213 (1995).
- ²³M. Du, X. Xie, Y. Jia, L. Mets, and G. R. Fleming, *Chem. Phys. Lett.* **201**, 535 (1993); M. Du, X. Xie, L. Mets, and G. R. Fleming, *J. Phys. Chem.* **98**, 4736 (1994); S. E. Bradforth, R. Jimenez, F. von Mourik, R. van Grondelle, and G. R. Fleming, *ibid.* **99**, 16 179 (1995).
- ²⁴L. O. Pålsson, S. E. Tjus, B. Andersson, and T. Gillbro, *Chem. Phys.* **194**, 291 (1995).
- ²⁵N. S. Reddy, H. van Amerongen, S. L. Kwa, R. van Grondelle, and G. J. Small, *J. Phys. Chem.* **98**, 4729 (1994).
- ²⁶S. Savikhin, Y. Zhu, S. Lin, R. E. Blankenship, and W. S. Struve, *J. Phys. Chem.* **98**, 10 322 (1994); M. Chachisvilis, H. Fidder, T. Pullerits, and V. Sundström, *J. Raman Spectr.* **26**, 513 (1995).
- ²⁷T. Joo, Y. Jia, J. Y. Yu, D. M. Jonas, and G. R. Fleming, *J. Phys. Chem.* (in press).
- ²⁸R. A. Marcus and N. Sutin, *Biochim. Biophys. Acta* **811**, 265 (1985).
- ²⁹H. Haken and G. Strobl, *Z. Phys.* **262**, 135 (1973).
- ³⁰R. Silbey, *Annu. Rev. Phys. Chem.* **27**, 203 (1976).
- ³¹P. Reineker, in *Exciton Dynamics in Molecular Crystals and Aggregates* (Springer-Verlag, Berlin, 1982), p. 111.
- ³²S. Mukamel, D. S. Franchi, and R. F. Loring, *Chem. Phys.* **128**, 99 (1988).
- ³³M. Cho, G. R. Fleming, and S. Mukamel, *J. Chem. Phys.* **98**, 5314 (1993).
- ³⁴M. Cho, G. R. Fleming, S. Saito, I. Ohmine, and R. M. Stratt, *J. Chem. Phys.* **100**, 6672 (1994).
- ³⁵Y. Tanimura and S. Mukamel, *J. Chem. Phys.* **99**, 9496 (1993).
- ³⁶P. More and T. Keyes, *Proceedings of the XXII Winter Meeting on Statistical Physics*, Cuernavaca, Mexico, 1994.
- ³⁷T. Holstein, *Ann. Phys. NY*, **8**, 325 (1959).
- ³⁸Y. Zhao, P. W. Brown, and W. K. Lindenberg, *J. Lumin.* **58**, 61 (1994); **60**, 762 (1994).
- ³⁹E. I. Rashba and M. D. Sturge, in *Excitons* (North-Holland, Amsterdam, 1982).
- ⁴⁰M. Ueta, H. Kanzaki, K. Kobayashi, Y. Toyozawa, and E. Hanamura, *Excitonic Processes in Solids* (Springer-Verlag, Berlin, 1986).
- ⁴¹J. Singh, *Excitation Energy Transfer Processes in Condensed Matter* (Plenum, New York, 1994).
- ⁴²S. Skourtis and S. Mukamel, *Chem. Phys.* **197**, 367 (1995).
- ⁴³S. Mukamel, *Principles of Nonlinear Optical Spectroscopy* (Oxford, New York, 1995).
- ⁴⁴M. Sparpaglione and S. Mukamel, *J. Chem. Phys.* **88**, 3263 (1988).
- ⁴⁵S. Mukamel and V. Rupasov, *Chem. Phys. Lett.* **242**, 17 (1995).
- ⁴⁶A. S. Davydov, *Theory of Molecular Excitons* (Plenum, New York, 1971).
- ⁴⁷Equation (28), together with Eq. (10), gives the fluorescence of molecule 1 (no energy transfer). This compact expression contains only a single term. When the problem is calculated in Liouville space it contains three terms representing fluorescence and Raman processes (see Chap. 9 of Ref. 43). The two expressions are identical. The Liouville space form has more terms since it contains a complete bookkeeping of the time ordering of the various interactions. The Liouville space form will be used in Sec. V.
- ⁴⁸ B_n in this case obeys Fermi statistics: $[B_n^+, B_n]_+ = 1$. This difference from Eq. (3) does not affect the quantities calculated here, since we consider only single-particle states.
- ⁴⁹R. Zwanzig, *J. Chem. Phys.* **33**, 1338 (1960).
- ⁵⁰V. M. Kenkre, in *Exciton Dynamics in Molecular Crystals and Aggregates* (Springer-Verlag, Berlin, 1982), p. 1.
- ⁵¹Th. Förster, *Ann. Phys. Leipzig (b)* **2**, 55 (1948); in *Modern Quantum Chemistry*, edited by O. Sinanoglu (Academic, New York, 1965), Vol. III, p. 93.
- ⁵²H. M. McConnell, *J. Chem. Phys.* **35**, 508 (1961).
- ⁵³M. Abramowitz and I. A. Stegun, *Handbook of Mathematical Functions* (Dover, New York, 1964).